Geophysical Research Letters

RESEARCH LETTER
10.1029/2023GL103165

Key Points:

- Relative contributions of mixed layer depth (MLD) and surface heat flux anomalies to sea surface temperature (SST) variability are investigated using the Flux Divergence Angle metric
- MLD anomalies tend to amplify SST anomalies in the extra-tropics, especially in eastern part of ocean basin, during the spring and summer
- MLD anomalies tend to suppress SST anomalies in the eastern tropical Pacific during December-January-February

Supporting Information:

Supporting Information may be found in the online version of this article.

Correspondence to:

N. Takahashi,
naoyat@hawaii.edu

Citation:

Takahashi, N., Richards, K. J., Schneider, N., Stuecker, M. F., Annamalai, H., & Nonaka, M. (2023). Observed relative contributions of anomalous heat fluxes and effective heat capacity to sea surface temperature variability. *Geophysical Research Letters*, *50*, e2023GL103165. https://doi.org/10.1029/2023GL103165

Received 13 FEB 2023
Accepted 21 JUL 2023

Observed Relative Contributions of Anomalous Heat Fluxes and Effective Heat Capacity to Sea Surface Temperature Variability

Naoya Takahashi[1], Kelvin J. Richards[1,2], Niklas Schneider[1,2], Malte F. Stuecker[1,2], Hariharasubramanian Annamalai[1,2], and Masami Nonaka[3]

[1]International Pacific Research Center, School of Ocean and Earth Science and Technology, University of Hawai'i at Mānoa, Honolulu, HI, USA, [2]Department of Oceanography, School of Ocean and Earth Science and Technology, University of Hawai'i at Mānoa, Honolulu, HI, USA, [3]Japan Agency for Marine-Earth Science and Technology, Yokohama, Japan

Abstract Sea surface temperatures (SSTs) vary not only due to heat exchange across the air-sea interface but also due to changes in effective heat capacity as primarily determined by mixed layer depth (MLD). Here, we investigate seasonal and regional characteristics of the contribution of MLD anomalies to the month-to-month variability of SST using observational datasets. First, we propose a metric called Flux Divergence Angle, which can quantify the relative contributions of surface heat fluxes and MLD anomalies to SST variability. Using this metric, we find that MLD anomalies tend to amplify SST anomalies in the extra-tropics, especially in the eastern ocean basins, during spring and summer. In contrast, MLD anomalies tend to suppress SST anomalies in the eastern tropical Pacific during December-January-February. This paper provides the first global picture of the observed importance of MLD anomalies to the local SST variability.

Plain Language Summary Sea surface temperature (SST) is one of the important indicators as well as drivers of climate variability over the globe. SST varies not only due to changes in surface heat fluxes but also due to changes in effective heat capacity as mainly determined by mixed layer depth (MLD). However, the observed characteristics of the latter process associated with the MLD anomalies are limited. In this study, we propose a new metric called "Flux Divergence Angle (FDA)," which can quantify the relative importance of MLD and surface heat flux to the SST variability. Using this metric, we find that the MLD anomalies tend to amplify the local SST variability in the extra-tropics during spring and summer. On the other hand, MLD anomalies tend to suppress the SST variability in the eastern tropical Pacific during December-January-February. This paper provides, for the first time, the global picture of relative importance of MLD anomalies to the SST variability based on observations.

1. Introduction

Sea surface temperature (SST) is one of the key metrics as well as drivers of climate variability over the globe. Surface heat flux is known as the most fundamental factor causing local SST variations in most of the extra-tropics (Frankignoul & Hasselmann, 1977; Hasselmann, 1976). Mixed layer depth (MLD) is in turn another key factor determining the effective heat capacity of the ocean surface layer, which also affects local SST variations (e.g., Alexander & Penland, 1996; Alexander et al., 2000; Amaya et al., 2021; Morioka et al., 2011; Qiu & Kelly, 1993; Takahashi et al., 2021; Yamamoto et al., 2020; Yokoi et al., 2012). More specifically, positive SST anomalies can be caused without the surface heat flux anomaly, if the mixed layer is shallower than usual with climatological heating (and vice versa). Therefore, not only the flux of heat across the air-sea interface is important, but also how this heat is re-distributed within the mixed layer.

Based on a mixed layer temperature budget from in-situ observations, previous studies have shown that shallow MLD anomalies can cause positive SST anomalies especially in spring and summer when MLD is shallow and climatological surface heating exists (Alexander & Penland, 1996; Alexander et al., 2000; Cronin et al., 2013; Elsberry & Garwood, 1978; Lanzante & Harnack, 1983). A part of the role of MLD anomalies has been revealed, however, a global picture of the relative importance of MLD anomalies in SST variability is missing. In the present, details of the role of MLD can be assessed with the availability of global observational datasets for three-dimensional oceanic properties. For example, Tozuka et al. (2018) proposed a metric for the relative importance of the surface heat flux and MLD anomalies to frontogenesis and frontolysis respectively based on Argo

float data, finding that seasonal variations of the horizontal gradient of MLD strongly contribute to the strength of the SST front. In the present study, we revisit the relative importance of surface heat flux and MLD anomalies to SST variability and explore their seasonal and regional characteristics over the global oceans.

The key scientific questions are "How large is the contribution of MLD anomalie to SST variability compared to the contribution of surface heat flux anomalies?" and "When/Where are they most important?." To answer these questions, we (a) propose a metric for quantifying the relative contributions of surface heat flux and MLD anomalies to the month-to-month variations of local SST anomalies and (b) reveal their seasonal (e.g., summer vs. winter) and regional characteristics (e.g., tropics vs. extra-tropics).

The remainder of the paper is organized as follows. In Section 2, we describe the datasets used in this study, and propose a metric to quantify the relative contributions of surface heat flux and MLD anomalies to local SST variability. In Section 3, we present the results on seasonality and regionality of the contribution of MLD anomaly. In Section 4, we summarize our results and discuss the possible role of MLD anomalies in major climate modes.

2. Data Sets and Methods

2.1. Data Sets

In this study, we utilize three variables; SST, surface heat fluxes, and MLD. Each variable is obtained from observational data sources; CERES-EBAF (Loeb et al., 2018) for radiative fluxes, OAFlux (Yu et al., 2008) for turbulent heat fluxes, OISST (Reynolds et al., 2002) for SST, and IPRC-Argo products (http://apdrc.soest.hawaii.edu/projects/argo/) for MLD. MLD is defined as the depth at which density increases by around 0.05 kg/m^3 from 10-m. The density increase is equivalent to a temperature decrease of 0.2°C. All variables are monthly-averaged, for 15 years from January 2005 to December 2019. The horizontal resolution of all variables is 1° in both zonal and meridional directions. Note that our results remain robust when using a shorter data period (e.g., January 2010 to December 2019) that excludes the sparsely distributed Argo profiles in the 2000s. The results are also not overly sensitive to the choice of data set used or the definition of MLD using a smaller density changes, for example, MILA-GPV product (Hosoda et al., 2010).

2.2. Metric to Determine the Relative Contributions of the Surface Heat Flux and MLD Anomalies to Local SST Variability

Here, we propose a metric to quantify the relative contributions of the surface heat flux and MLD anomalies to local SST variability. We start to develop the metric from the simplified mixed layer temperature budget equation (Moisan & Niiler, 1998) considering only surface forcing:

$$\frac{\partial T}{\partial t} = \frac{Q}{\rho c_p H} + \varepsilon_o, \tag{1}$$

where ρ is the density of sea water, c_p is the specific heat capacity at constant pressure, H is MLD, and ε_o is the sum of contributions from all other oceanic processes not explicitly written in the equation (e.g., three-dimensional advection, entrainment, and diffusion) and observational error. T is vertical mean temperature within the mixed layer. In this study, we assume that T is equivalent to SST. Q is the surface heat flux into the mixed layer and calculated as the difference between net surface heat flux (Q_0) and penetrative shortwave radiation at the bottom of mixed layer (q_{pen}): $Q = Q_0 - q_{\mathrm{pen}}$. The q_{pen} is calculated following Paulson and Simpson (1977). Hereafter, we focus on month-to-month SST variations and define anomalies of all variables as the deviations from the monthly climatology at each grid point. Considering the heat budget equation for T anomalies, we can decompose the anomalies of the first term on the right-hand-side (rhs) of Equation 1 into contributions from the surface heat flux and MLD anomalies (Alexander & Penland, 1996; Morioka et al., 2010; Yokoi et al., 2012). We rewrite the heat budget equation for the anomaly field:

$$\frac{\partial T'}{\partial t} \sim \frac{Q'}{\rho c_p \overline{H}} - \frac{\overline{Q} H'}{\rho c_p \overline{H}^2} + \varepsilon_o', \tag{2}$$

where overbars ($\overline{X}$) and primes (X') denote the monthly climatology and anomalies, respectively. The first term on the rhs represents the contribution of the surface heat flux anomalies (Q') acting on a climatological MLD ($\overline{H}$) and the second term represents the contribution of the MLD anomalies (H') under climatological heating/cooling ($\overline{Q}$). We ignore second and higher order terms of the Taylor Expansion in Equation 2 (e.g., the non-linear

contribution of both anomalies) because they are typically much smaller than the sum of the first two terms (~1/10), except in the Antarctic Circumpolar Current region and the Labrador Sea where the subduction zone of the Atlantic Meridional Overturning Circulation is located. The first two terms can explain more than 90% of the total variances of the surface forcing term in most of the region (Figure S1 in Supporting Information S1).

Next, we formulate a temperature variance budget equation (Boucharel et al., 2015; Guan et al., 2019; Santoso et al., 2010) by multiplying the SST anomaly (T') on both sides of Equation 2:

$$T'\frac{\partial T'}{\partial t} = T'\left(\frac{Q'}{\rho c_p \overline{H}} - \frac{\overline{Q}H'}{\rho c_p \overline{H}^2} + \varepsilon_o{}'\right), \tag{3}$$

$$\frac{1}{2}\frac{\partial (T')^2}{\partial t} = \frac{1}{\rho c_p \overline{H}}\left(Q'T' - H'\frac{\overline{Q}}{\overline{H}}T'\right) + \varepsilon_o{}'T'. \tag{4}$$

The left-hand-side of the equations are equivalent to half of the time tendency of T' squared, hence we can diagnose the dominant processes that result in an increase or decrease of the T' squared. The reason why we employ the variance budget equation (Equation 4) instead of the heat budget equation (Equation 2) is that the role of surface forcing processes in the SST evolution can be captured by the variance budget equation.

As noted in Section 1, Tozuka et al. (2018) proposed a metric for quantifying the relative contribution of horizontal gradients of the surface heat flux and MLD to the seasonal variation of frontogenesis. A similar metric was also applied to the sea surface salinity front (Ohishi et al., 2019). The method is analogous to the Turner angle (Ruddick, 1983; You, 2002) which can be used to diagnose relative contributions of vertical gradients of temperature and salinity to double-diffusive convection. Here, following the basic concepts of these studies, we define a new metric called the Flux Divergence Angle (FDA; Θ), which quantifies the relative contributions of surface heat flux and MLD anomalies to local SST variability, in terms of the four-quadrant arctangent function, namely:

$$\Theta = \tan^{-1}(Q_Q - Q_H, Q_Q + Q_H), \tag{5}$$

where

$$Q_Q = Q'T', \qquad Q_H = -H'\frac{\overline{Q}}{\overline{H}}T'.$$

(Note, $\tan^{-1}(x, y) = \tan^{-1}(y/x)$, with the angle dependent on the sign of both x and y.) The two indices of Q_Q and Q_H are a part of the Equation 4, have the same unit of °C*W/m^2, and represent the product of anomalies of SST and surface heat flux (or the product of anomalies of SST and equivalent heat flux anomalies due to the MLD anomaly with climatological heating/cooling). Positive and negative values of these indices represent that the heat flux anomalies amplify and dampen the local SST anomalies, respectively. Note that the term of "FDA" was selected to describe the role of the MLD and surface heat flux in modulating the divergence of the heat flux within the mixed layer. Figures 1a–1c are snapshots of SST, surface heat flux, and MLD anomalies on June 2015. In addition, a snapshot of FDA on June 2015 is shown in Figure 1d, calculated via Equation 5 at each grid point. Figure 1f shows a two-dimensional histogram of all pairs of Q_Q and Q_H, showing that there is no apparent linear relationship between them (e.g., correlation coefficient of all pairs of Q_Q and Q_H: $r = -0.11$).

Next, we illustrate the physical meaning of the FDA using a schematic in Figure 1e. When the FDA has a positive value (i.e., when the sum of Q_Q and Q_H is positive), the product of total surface forcing and SST anomaly is positive, so that the surface forcing term in Equation 4 acts to amplify the local SST anomalies. This is referred to as "Growth" stage of the SST evolution by surface forcing. Analogous, when the FDA has a negative value (i.e., when the sum of Q_Q and Q_H is negative), the product of total surface forcing and SST anomaly is negative, so that the surface forcing term in Equation 4 acts to dampen the local SST anomalies ("Decay" stage). Additionally, when the contribution of the surface heat flux is larger than that of MLD, FDA has a specific value range of $0° < \Theta < 90°$ for the "Growth" stage and $-180° < \Theta < -90°$ for the "Decay" stage. In contrast, when the contribution of MLD is larger than that of the surface heat flux, FDA has the range of $90° < \Theta < 180°$ for the "Growth" and $-90° < \Theta < 0°$ for the "Decay" stage. Depending on the relative importance, we add the header of "Q_Q" or "Q_H" before the name of "Growth" or "Decay" stage (e.g., "Q_Q Growth" when $0° < \Theta < 90°$). Note that a term of "*dominant*" in the following text indicates their relative importance of the surface heat flux and MLD terms but not necessarily their absolute importance relative to other terms in the full variance heat budget. For

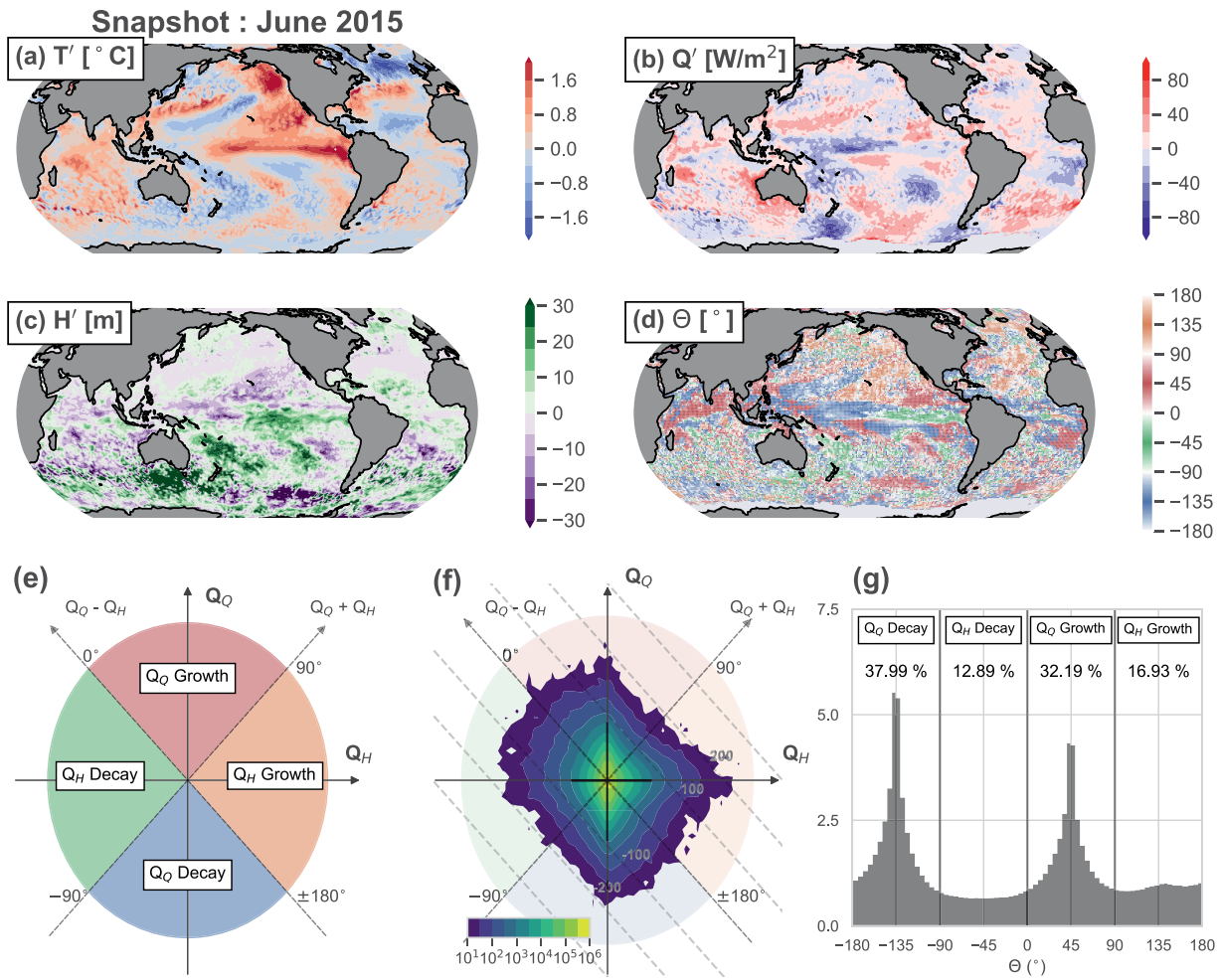

Figure 1. Snapshots of horizontal maps of (a) SST anomaly, (b) surface heat flux anomaly, (c) mixed layer depth anomaly, and (d) Flux Divergence Angle (FDA) on June 2015. Note that white color in (d) indicates the value near the boundary of each sector. (e) Schematic diagram of the four sectors ("Q_Q Decay"/"Q_H Decay"/"Q_Q Growth"/"Q_H Growth") diagnosed by the FDA metric. (f) Two-dimensional histogram of Q_Q and Q_H using all pairs over the global ocean and in all seasons. Units of Q_Q and Q_H are °C*W/m^2. Bin size is 10°C*W/m^2 for both Q_Q and Q_H. Only count numbers greater than 10 are displayed. Dashed contours where $Q_Q + Q_H = -300, -200, -100, 0, 100, 200, 300$ are also plotted. (g) Histogram of FDA normalized by total count numbers (Unit: %) using a bin size of 5°. Thick vertical lines in Figure 1g indicate the boundary between each sector. Numbers below each label indicate the occurrence frequency in each sector (Unit: %).

example, oceanic processes associated with upwelling and lateral advection have large impacts on SST variability in the eastern tropical Pacific and in western boundary current regions, respectively (Figure S2 in Supporting Information S1). Also, the oceanic processes tend to be the primary driver of local SST variability in the winter hemisphere (Figure S3 in Supporting Information S1). In such cases, surface forcing processes are less important than oceanic processes. Hence, the term "*dominant*" used in this manuscript refers to only the relative importance of the surface heat flux anomaly or MLD anomaly among the surface forcing processes.

To further investigate the regional characteristics of the FDA histogram (Figure 1g), we calculate the occurrence frequencies of the four sectors (F_i) at each grid point during specific seasons as below,

$$F_i(x,y) = \frac{N_i(x,y)}{N_{\mathrm{ALL}}}, \begin{cases} i=1: & -180^\circ \le \Theta < -90^\circ \\ i=2: & -90^\circ \le \Theta < 0^\circ \\ i=3: & 0^\circ \le \Theta < 90^\circ \\ i=4: & 90^\circ \le \Theta < 180^\circ \end{cases} \quad (6)$$

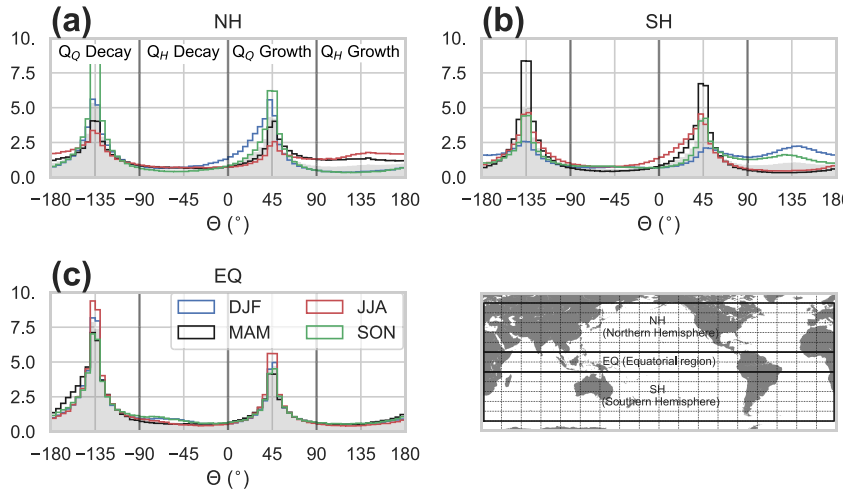

Figure 2. Normalized histograms of Flux Divergence Angle (Unit: %) in 3 selected regions (a. Northern Hemisphere [NH: 10°N–60°N], b. Southern Hemisphere [SH: 10°S–60°S], and c. Equatorial region [EQ: 10°S–10°N]). Each color indicates the results for each season separately (December-January-February [DJF, blue], March-April-May [MAM, black], June-July-August [JJA, red], and September-October-November [SON, green], All season [gray filled]). Bin size of the histograms is 5°. Thick vertical line in each panel indicates the boundary between each sector. The map in lower right corner indicates the area of each selected region.

where N_i is the count number of events with a specific value range of FDA. N_{ALL} is the total count number at one grid point, which is 45 for each season (i.e., each 3-month seasonal average during 15 years). Horizontal maps of F_i tell us the regionality of the dominant processes for the local SST evolution at each grid point.

3. Results

3.1. Global Characteristics of FDA

First, we provide an overview of the general characteristics of the FDA over the global ocean and in all seasons. Figure 1g shows a histogram of FDAs normalized by total count numbers. The number below each label indicates the occurrence frequency of each sector. The histogram has two sharp peaks at around 45° and −135°. The occurrence frequency of "Q_Q Growth" is 32.19% and that of "Q_Q Decay" is 37.99%. These results demonstrate that surface heat flux anomalies are the main factor determining anomalies of the total surface forcing term. This is consistent with previous results on the relationship between the surface heat flux and SST, that is, SST anomalies can be caused by wind or radiative forcing and can be dampened by heat release from the sea surface (Hasselmann, 1976). Although the surface heat flux anomalies are the main driver of the SST anomalies in most of the cases investigated here, in some cases MLD anomalies contribute more to the SST anomalies than the surface heat flux anomalies. For example, FDA around Hawaii on June 2015 (Figure 1d) had positive values greater than 90° (i.e., orange color shading), suggesting that the SST anomalies were primarily determined by the "Q_H Growth" process rather than "Q_Q Growth" and "Q_Q Decay." In the next subsection, we further explore the regional and seasonal characteristics of the "Q_H Growth" and "Q_H Decay" processes.

3.2. Regional and Seasonal Characteristics of FDA

Figure 2 shows the FDA histograms for different regions (Northern Hemisphere, Equatorial region, and Southern Hemisphere), and different seasons (December-January-February [DJF], March-April-May [MAM], June-July-August [JJA], and September-October-November [SON]). Maps of the occurrence frequencies of the four sectors in each season are also shown in Figure 3. As described in the previous subsection, the contribution of surface heat flux anomalies is dominant all over the global ocean (Figure 2), especially in most of the extra-tropical regions and in winter (Figures 3a, 3c, 3e, 3g, 3i, 3k, 3m, and 3o). Hereafter, we will describe the details of the contributions of MLD anomalies (i.e., "Q_H Growth" and "Q_H Decay") compared to the contribution of surface heat flux anomalies (i.e., "Q_Q Growth" and "Q_Q Decay").

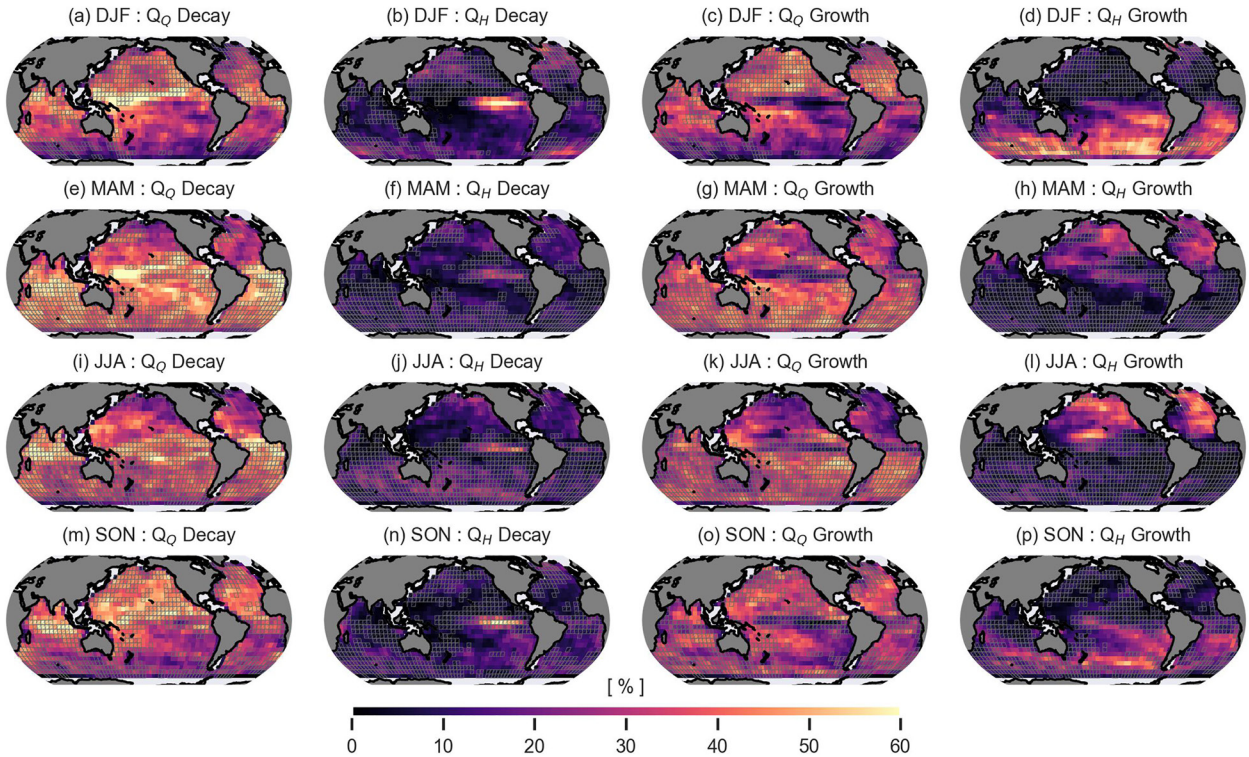

Figure 3. Horizontal maps of occurrence frequencies (Unit: %) in the four sectors for each season. From left to right, the "Q_Q Decay," "Q_H Decay," "Q_Q Growth," and "Q_H Growth" sectors are displayed, respectively. Each row shows the results in DJF (1st row), MAM (2nd row), JJA (3rd row), and SON (4th row). Light gray hatches indicate the grid where relative contribution of surface forcing term is *not* the primary driver of T variability (i.e., linear regression coefficient of surface forcing term onto the total tendency term during each season [Figures S3a, S3c, S3e, and S3g in Supporting Information S1] is less than 0.5).

3.2.1. Q_H Growth Process: Contribution of MLD Anomalies to the Growth of SST Anomalies

In the extra-tropics (Figures 2a and 2b), the histograms show a clear seasonal difference between summer and winter. In the winter hemisphere (i.e., DJF in the Northern Hemisphere and JJA in the Southern Hemisphere), occurrence frequencies of "Q_Q Growth" and "Q_Q Decay" are larger than those of "Q_H Growth" and "Q_H Decay." In the summer hemisphere (i.e., JJA in the Northern Hemisphere and DJF in the Southern Hemisphere), the surface forcing term is the primary driver of extra-tropical SST variability (Figure S3 in Supporting Information S1). Occurrence frequencies of "Q_Q Growth" and "Q_Q Decay" are also large in spring and summer, however, the occurrence frequency of "Q_H Growth" is clearly larger than that in winter. This suggests that the contribution of MLD anomalies is more pronounced in the spring and summer seasons than in the winter season, which is consistent with previous research (Alexander & Penland, 1996; Alexander et al., 2000; Cronin et al., 2013; Elsberry & Garwood, 1978; Lanzante & Harnack, 1983). The "Q_H Growth" sector reflects the negative product of anomalies of SST and MLD under climatological heating. In this situation, SST easily increases under a shallow MLD anomaly and climatological surface heating in the summer hemisphere.

As noted in the previous paragraph, the "Q_H Growth" sector is dominant in the summer hemisphere, particularly in the eastern part of the ocean basins (Figures 3d, 3h, 3l, and 3p). The region with a large contribution of MLD anomalies exhibits a horseshoe-like pattern, especially in the North Pacific (Figures 3h and 3l). One reason for the large contribution of MLD anomalies is large variability of MLD anomalies in subtropical regions (Figure S4a in Supporting Information S1), particularly due to strong surface friction velocity in the subtropical Pacific (Zhu & Zhang, 2018). Another reason is a large value of the ratio of the mean surface heat flux to mean MLD in the North Pacific and Atlantic (>50°N in Figure S4b in Supporting Information S1), which is mainly due to the shallow climatological mean MLD under the strong climatological heating at the sea surface during the summer (Figures S4c and S4d in Supporting Information S1).

3.2.2. Q_H Decay Process: Contribution of MLD Anomalies to the Decay of SST Anomalies

Tropical SST variability is primarily driven by the oceanic term rather than the surface forcing term (Figures S2 and S3 in Supporting Information S1). However, the thermal damping process described as the surface forcing term play a crucial role in the decaying phase of El Niño-Southern Oscillation (e.g., Boucharel et al., 2015; Guan et al., 2019; Timmerman et al., 2018). Histogram of FDA in the tropics (Figure 2c) shows that the contribution of surface heat flux anomalies is basically dominant. In addition, occurrence frequency of "Q_H Decay" is slightly larger in SON and DJF than in other seasons. Horizontal maps of the "Q_H Decay" occurrence frequency (Figures 3b, 3f, 3j, and 3n) show that this process is dominant in the eastern tropical Pacific during DJF. The "Q_H Decay" sector reflects the positive product of anomalies of SST and MLD under climatological heating. It is consistent with the regionality of positive covariance between anomalies of SST and MLD in the oceanic upwelling zone (Carton et al., 2008; Cronin & Kessler, 2002; Huang et al., 2012; Wang & McPhaden, 2000), resulting in negative anomalies of equivalent heat flux with deeper MLD under climatological heating in the tropics that act to dampen positive SST anomalies. Although there are various important processes that modulate the MLD anomaly in the tropics, such as wind stirring, surface buoyancy forcing derived from fresh water flux, and lateral advection (e.g., Pookkandy et al., 2016), we will not further discuss the formation mechanism of the MLD anomaly.

4. Summary and Discussion

To reveal the seasonal and regional characteristics of the role of MLD anomalies in modulating SST variability, we propose a metric called FDA that quantifies the relative contributions of surface heat flux and MLD anomalies to the month-to-month variations of SST anomalies. The FDA is defined in terms of the four-quadrant arctangent function and based on a metric proposed by Tozuka et al. (2018). Using the FDA, we investigate the seasonal and regional characteristics of their relative contributions. The contribution of MLD anomalies has two distinct features. First, MLD anomalies amplify local SST anomalies particularly in the extra-tropics during spring and summer, relative to the contribution of surface heat flux anomalies. Second, MLD anomalies suppress local SST anomalies particularly in the eastern part of the tropical Pacific during DJF. This paper provides the first global picture of the relative importance of surface heat flux and MLD anomalies to the local SST variability based on observational datasets.

Our results show that the spatial pattern with pronounced contributions of MLD anomalies in the North Pacific during spring and summer is horseshoe-like (Figure 3). This implies that MLD anomalies might play a critical role in modulating the climate variability in the North Pacific. Recent papers pointed out the importance of MLD anomalies in modulating major modes of climate variability such as the Pacific Decadal Oscillation (Dawe & Thompson, 2007), Atlantic Meridional Mode (Kataoka et al., 2019), and the Atlantic Multidecadal Oscillation (Yamamoto et al., 2020). Kataoka et al. (2019) also revealed that variations in MLD have the potential to more than double the wind-evaporation-SST feedback rate. Thus, the role of MLD anomalies in climate variability should be paid more attention to and its further investigation is needed.

Although our results demonstrate the observed contribution of MLD anomalies to the local SST variability, it is widely recognized that large uncertainties associated with summertime MLD exist in ocean and coupled general circulation models (Ezer, 2000; Huang et al., 2014). The presence of MLD biases in climate models is a potential source of SST biases (Zhu et al., 2020). Thus, improved understanding of the different formation mechanisms of MLD anomalies is required, especially for physical processes associated with the MLD variability driven by wind stirring, surface buoyancy forcing derived from fresh water flux, and lateral advection (Lee et al., 2015; Pookkandy et al., 2016; Ushijima & Yoshikawa, 2019; Yoshikawa, 2015). Furthermore, quantifying the feedback process between SST and MLD via aforementioned physical processes would be valuable. Finally, we highlight that our simple metric based on only three variables is a useful diagnostic when considering the representation of the upper ocean in climate models.

Data Availability Statement

Most of the datasets used in this study can be downloaded from Asia-Pacific Data Research Center; http://apdrc.soest.hawaii.edu/data/data.php, which is a part of the International Pacific Research Center at the University of Hawai'i at Mānoa, funded in part by the National Oceanic and Atmospheric Administration (NOAA). Original

data sources are listed below; OISSTv2 is from https://www.ncei.noaa.gov/products/optimum-interpolation-sst. CERES data were obtained from the NASA Langley Research Center CERES ordering tool at https://asdc.larc.nasa.gov/project/CERES/CERES_EBAF_Edition4.1. The global ocean heat flux and evaporation data provided by the Woods Hole Oceanographic Institution OAFlux project (https://oaflux.whoi.edu/data-access/) were funded by the NOAA Climate Observations and Monitoring (COM) program.

Acknowledgments
This study was supported by the JAMSTEC and IPRC Collaborative Research (JICore) project and in part by the Office of Naval Research through the Climate Resilience Collaborative at the University of Hawai'i at Mānoa. MFS was supported by NSF Grant AGS-2141728 and NOAA's Climate Program Office's Modeling, Analysis, Predictions, and Projections (MAPP) program Grant NA20OAR4310445. HA acknowledges the partial support from NOAA/MAPP program Grants NA18OAR4310279 and NA21OAR4310348. This is IPRC publication No.1605 and SOEST contribution No.11698. Finally, the authors are grateful for the thoughtful comments of three anonymous reviewers that improved the original manuscripts.

References

Alexander, M. A., & Penland, C. (1996). Variability in a mixed layer ocean model driven by stochastic atmospheric forcing. *Journal of Climate*, *9*(10), 2424–2442. https://doi.org/10.1175/1520-0442(1996)009<2424:VIAMLO>2.0.CO;2

Alexander, M. A., Scott, J. D., & Deser, C. (2000). Processes that influence sea surface temperature and ocean mixed layer depth variability in a coupled model. *Journal of Geophysical Research*, *105*(C7), 16823–16842. https://doi.org/10.1029/2000jc900074

Amaya, D. J., Alexander, M. A., Capotondi, A., Deser, C., Karnauskas, K. B., Miller, A. J., & Mantua, N. J. (2021). Are long-term changes in mixed layer depth influencing North Pacific marine heatwaves? *Bulletin of the American Meteorological Society*, *102*(1), S59–S66. https://doi.org/10.1175/BAMS-D-20-0144.1

Boucharel, J., Timmermann, A., Santoso, A., England, M. H., Jin, F., & Balmaseda, M. A. (2015). A surface layer variance heat budget for ENSO. *Geophysical Research Letters*, *42*(9), 3529–3537. https://doi.org/10.1002/2015GL063843

Carton, J. A., Grodsky, S. A., & Liu, H. (2008). Variability of the oceanic mixed layer, 1960–2004. *Journal of Climate*, *21*(5), 1029–1047. https://doi.org/10.1175/2007JCLI1798.1

Cronin, M. F., Bond, N. A., Thomas Farrar, J., Ichikawa, H., Jayne, S. R., Kawai, Y., et al. (2013). Formation and erosion of the seasonal thermocline in the Kuroshio extension recirculation gyre. *Deep Sea Research Part II: Topical Studies in Oceanography*, *85*, 62–74. https://doi.org/10.1016/j.dsr2.2012.07.018

Cronin, M. F., & Kessler, W. S. (2002). Seasonal and interannual modulation of mixed layer variability at 0°, 110°W. *Deep Sea Research Part I: Oceanographic Research Papers*, *49*(1), 1–17. https://doi.org/10.1016/S0967-0637(01)00043-7

Dawe, J. T., & Thompson, L. A. (2007). PDO-related heat and temperature budget changes in a model of the North Pacific. *Journal of Climate*, *20*(10), 2092–2108. https://doi.org/10.1175/JCLI4229.1

Elsberry, R. L., & Garwood, R. W. (1978). Sea-surface temperature anomaly generation in relation to atmospheric storms. *Bulletin of the American Meteorological Society*, *59*(7), 786–789. https://doi.org/10.1175/1520-0477(1978)059<0786:SSTAGI>2.0.CO;2

Ezer, T. (2000). On the seasonal mixed layer simulated by a basin-scale ocean model and the Mellor-Yamada turbulence scheme. *Journal of Geophysical Research*, *105*(C7), 16843–16855. https://doi.org/10.1029/2000JC900088

Frankignoul, C., & Hasselmann, K. (1977). Stochastic climate models, part II application to sea-surface temperature anomalies and thermocline variability. *Tellus*, *29*(4), 289–305. https://doi.org/10.3402/tellusa.v29i4.11362

Guan, C., McPhaden, M. J., Wang, F., & Hu, S. (2019). Quantifying the role of oceanic feedbacks on ENSO asymmetry. *Geophysical Research Letters*, *46*(4), 2140–2148. https://doi.org/10.1029/2018GL081332

Hasselmann, K. (1976). Stochastic climate models part I. Theory. *Tellus*, *28*(6), 473–485. https://doi.org/10.3402/tellusa.v28i6.11316

Hosoda, S., Ohira, T., Sato, K., & Suga, T. (2010). Improved description of global mixed-layer depth using Argo profiling floats. *Journal of Oceanography*, *66*(6), 773–787. https://doi.org/10.1007/s10872-010-0063-3

Huang, B., Xue, Y., Wang, H., Wang, W., & Kumar, A. (2012). Mixed layer heat budget of the El Niño in NCEP climate forecast system. *Climate Dynamics*, *39*(1–2), 365–381. https://doi.org/10.1007/s00382-011-1111-4

Huang, C. J., Qiao, F., & Dai, D. (2014). Evaluating CMIP5 simulations of mixed layer depth during summer. *Journal of Geophysical Research: Oceans*, *119*(4), 2568–2582. https://doi.org/10.1002/2013JC009535

Kataoka, T., Kimoto, M., Watanabe, M., & Tatebe, H. (2019). Wind–mixed layer–SST feedbacks in a tropical air–sea coupled system: Application to the Atlantic. *Journal of Climate*, *32*(13), 3865–3881. https://doi.org/10.1175/JCLI-D-18-0728.1

Lanzante, J. R., & Harnack, R. P. (1983). An investigation of summer sea surface temperature anomalies in the eastern North Pacific Ocean. *Tellus A: Dynamic Meteorology and Oceanography*, *35*(4), 256–268. https://doi.org/10.3402/tellusa.v35i4.11438

Lee, E., Noh, Y., Qiu, B., & Yeh, S.-W. (2015). Seasonal variation of the upper ocean responding to surface heating in the North Pacific. *Journal of Geophysical Research: Oceans*, *120*(8), 5631–5647. https://doi.org/10.1002/2015JC010800

Loeb, N. G., Doelling, D. R., Wang, H., Su, W., Nguyen, C., Corbett, J. G., et al. (2018). Clouds and the Earth's radiant energy system (CERES) energy balanced and filled (EBAF) top-of-atmosphere (TOA) edition-4.0 data product. *Journal of Climate*, *31*(2), 895–918. https://doi.org/10.1175/JCLI-D-17-0208.1

Moisan, J. R., & Niiler, P. P. (1998). The seasonal heat budget of the North Pacific: Net heat flux and heat storage rates (1950–1990). *Journal of Physical Oceanography*, *28*(3), 401–421. https://doi.org/10.1175/1520-0485(1998)028<0401:tshbot>2.0.co;2

Morioka, Y., Tozuka, T., & Yamagata, T. (2010). Climate variability in the southern Indian Ocean as revealed by self-organizing maps. *Climate Dynamics*, *35*(6), 1059–1072. https://doi.org/10.1007/s00382-010-0843-x

Morioka, Y., Tozuka, T., & Yamagata, T. (2011). On the growth and decay of the subtropical dipole mode in the South Atlantic. *Journal of Climate*, *24*(21), 5538–5554. https://doi.org/10.1175/2011JCLI4010.1

Ohishi, S., Katsura, S., & Aiki, H. (2019). Salinity frontogenesis/frontolysis in the northeastern subtropical Pacific region. *Climate Dynamics*, *53*(9–10), 5927–5943. https://doi.org/10.1007/s00382-019-04907-w

Paulson, C. A., & Simpson, J. J. (1977). Irradiance measurements in the upper ocean. *Journal of Physical Oceanography*, *7*(6), 952–956. https://doi.org/10.1175/1520-0485(1977)007<0952:IMITUO>2.0.CO;2

Pookkandy, B., Dommenget, D., Klingaman, N., Wales, S., Chung, C., Frauen, C., & Wolff, H. (2016). The role of local atmospheric forcing on the modulation of the ocean mixed layer depth in reanalyses and a coupled single column ocean model. *Climate Dynamics*, *47*(9–10), 2991–3010. https://doi.org/10.1007/s00382-016-3009-7

Qiu, B., & Kelly, K. A. (1993). Upper-ocean heat balance in the Kuroshio extension region. *Journal of Physical Oceanography*, *23*(9), 2027–2041. https://doi.org/10.1175/1520-0485(1993)023<2027:UOHBIT>2.0.CO;2

Reynolds, R. W., Rayner, N. A., Smith, T. M., Stokes, D. C., & Wang, W. (2002). An improved in situ and satellite SST analysis for climate. *Journal of Climate*, *15*(13), 1609–1625. https://doi.org/10.1175/1520-0442(2002)015<1609:AIISAS>2.0.CO;2

Ruddick, B. (1983). A practical indicator of the stability of the water column to double-diffusive activity. *Deep-Sea Research, Part A: Oceanographic Research Papers*, *30*(10), 1105–1107. https://doi.org/10.1016/0198-0149(83)90063-8

Santoso, A., Sen Gupta, A., & England, M. H. (2010). Genesis of Indian Ocean mixed layer temperature anomalies: A heat budget analysis. *Journal of Climate*, *23*(20), 5375–5403. https://doi.org/10.1175/2010JCLI3072.1

Takahashi, N., Richards, K. J., Schneider, N., Annamalai, H., Hsu, W., & Nonaka, M. (2021). Formation mechanism of warm SST anomalies in 2010s around Hawaii. *Journal of Geophysical Research: Oceans*, *126*(11), 1–14. https://doi.org/10.1029/2021JC017763

Timmermann, A., An, S. I., Kug, J. S., Jin, F. F., Cai, W., Capotondi, A., et al. (2018). El Niño-Southern Oscillation complexity. *Nature*, *559*(7715), 535–545. https://doi.org/10.1038/s41586-018-0252-6

Tozuka, T., Ohishi, S., & Cronin, M. F. (2018). A metric for surface heat flux effect on horizontal sea surface temperature gradients. *Climate Dynamics*, *51*(1–2), 547–561. https://doi.org/10.1007/s00382-017-3940-2

Ushijima, Y., & Yoshikawa, Y. (2019). Mixed layer depth and sea surface warming under diurnally cycling surface heat flux in the heating season. *Journal of Physical Oceanography*, *49*(7), 1769–1787. https://doi.org/10.1175/JPO-D-18-0230.1

Wang, W., & McPhaden, M. J. (2000). The surface-layer heat balance in the Equatorial Pacific Ocean Part II: Interannual variability. *Journal of Physical Oceanography*, *30*(11), 2989–3008. https://doi.org/10.1175/1520-0485(2001)031<2989:TSLHBI>2.0.CO;2

Yamamoto, A., Tatebe, H., & Nonaka, M. (2020). On the emergence of the Atlantic multidecadal SST signal: A key role of the mixed layer depth variability driven by North Atlantic Oscillation. *Journal of Climate*, *33*(9), 3511–3531. https://doi.org/10.1175/JCLI-D-19-0283.1

Yokoi, T., Tozuka, T., & Yamagata, T. (2012). Seasonal and interannual variations of the SST above the Seychelles Dome. *Journal of Climate*, *25*(2), 800–814. https://doi.org/10.1175/JCLI-D-10-05001.1

Yoshikawa, Y. (2015). Scaling surface mixing/mixed layer depth under stabilizing buoyancy flux. *Journal of Physical Oceanography*, *45*(1), 247–258. https://doi.org/10.1175/JPO-D-13-0190.1

You, Y. (2002). A global ocean climatological atlas of the Turner angle: Implications for double-diffusion and water-mass structure. *Deep Sea Research Part I: Oceanographic Research Papers*, *49*(11), 2075–2093. https://doi.org/10.1016/S0967-0637(02)00099-7

Yu, L., Jin, X., & Robert, A. W. (2008). *Multidecade global flux datasets from the objectively analyzed air-sea fluxes (OAFlux) Project: Latent and sensible heat fluxes, ocean evaporation, and related surface meteorological variables*. Woods Hole Oceanographic Institution OA Flux Project Technical Report. (OA-2008-01). https://doi.org/10.1007/s00382-011-1115-0

Zhu, Y., & Zhang, R.-H. (2018). Scaling wind stirring effects in an oceanic bulk mixed layer model with application to an OGCM of the tropical Pacific. *Climate Dynamics*, *51*(5–6), 1927–1946. https://doi.org/10.1007/s00382-017-3990-5

Zhu, Y., Zhang, R.-H., & Sun, J. (2020). North Pacific upper-ocean cold temperature biases in CMIP6 simulations and the role of regional vertical mixing. *Journal of Climate*, *33*(17), 7523–7538. https://doi.org/10.1175/JCLI-D-19-0654.1